Photodegradation and Biodegradation by Bacteria of Mulching Films Based on Ethylene-Vinyl Acetate Copolymer: Effect of Pro-Oxidant Additives

C. Abrusci,[1] J. L. Pablos,[2] I. Marín,[1] E. Espí,[3] T. Corrales,[2] F. Catalina[2]

[1]*Departamento de Biología Molecular, Facultad de Ciencias, Universidad Autónoma de Madrid-UAM, Cantoblanco, Madrid 28049, Spain*
[2]*Polymer Photochemistry Group, Instituto de Ciencia y Tecnología de Polímeros, C.S.I.C., Juan de la Cierva 3, Madrid 28006, Spain*
[3]*Repsol, Ctra. A-5, Km. 18, 28931-Móstoles, Madrid, Spain*

Received 20 September 2011; accepted 10 February 2012
DOI 10.1002/app.36989
Published online in Wiley Online Library (wileyonlinelibrary.com).

ABSTRACT: The photodegradation (432 h under irradiation of Xe-Lamp-solar filter) of an ethylene vinyl acetate (EVA) copolymer with vinyl acetate content of 9% was studied, and the effect of iron and calcium stearates was evaluated using different techniques such us attenuated total reflectance-Fourier transform infrared spectroscopy (ATR-FTIR), gel permeation chromatography (GPC), and thermal analysis methods (DSC and TGA). A re-arrangement in crystallization and consequent decrease in thermal stability were found through differential scanning calorimetry (DSC) and thermogravimetric analysis (TGA), which were in agreement with the chain scission tendency. The presence of Ca and Fe pro-oxidants additives in EVA films increased the ketone carbonyl formation and decreased the ester absorption band of the acetate respect to the pure EVA, as it was evidenced by the significant changes in Carbonyl Indexes found by FTIR. The activity of stearates has been also evaluated by chemiluminescence, where the temperature-ramping tests under nitrogen showed the formation of a peroxide peak at lower temperature. The lower stability of the films containing pro-oxidants was evidenced by the values of oxidation induction time (OIT) determined by DSC. The results were supported by GC-MS, where the concentration of extracted products identified in the EVA containing pro-oxidants was significant and a much greater decrease in molecular weight was determined by GPC, which confirmed the development of degradation for EVA with Ca and Fe stearates in comparison to pure EVA. Biodegradation of photodegraded EVA films were studied at 45°C during 90 days using a mixture of *Bacillus* (MIX) (*B. cereus, B. megaterium*, and *B. subtilis*) and, in parallel, by *Brevibacillus borstelensis* as reference strain. Biodegradation of EVA-films was studied by Chemiluminescence, ATR-FTIR and GC-product analysis and the data confirm more efficient biodegradation on the materials containing pro-oxidants. The chemiluminescence emissions due to decomposition of oxidation species was observed at lower temperatures on the biodegraded samples. Also, the drastic decrease of carbonyl index and the disappearance of photogenerated low molecular products with biodegradation were more efficient on the biodegraded films containing pro-oxidants. EVA mineralization was evaluated by carbon dioxide measurement using indirect impedance technique. Biodegradation by *B. borstelensis* and MIX at 45°C was similar and exhibited a pronounced difference between the pure photodegraded EVA film (around 15% of mineralization) and the corresponding photodegraded films containing Ca and Fe stearates where biodegradation extent reached values of 23-26% of biodegradation after 90 days. J Appl Polym Sci 000: 000–000, 2012

Key words: ethylene-vinyl acetate copolymer (EVA); photodegradation; biodegradation; bacteria; pro-oxidants; agriculture

INTRODUCTION

Nowadays, polyethylene and its copolymers such us ethylene-vinyl acetate are the preferred materials in the application of agricultural films. The advantages of ethylene vinyl acetate copolymers[1] (EVA) against polyethylene as base polymer for agricultural films are determined by two intrinsic characteristics: its greater polarity and less crystallinity. The higher polarity of EVA results in more compatibility with the majority of organic additives than low density polyethylene (LDPE), which makes it have a better dispersion in the polymeric matrix, a slower migration and a higher maximum concentration. Because of this, film quality improves and a longer duration of an anti-drip effect is achieved. In test carried out in Florida (USA) and Almeria (Spain) or artificial ageing (xenon lamp Atlas Ci4000) it has been demonstrated that the photostability increases with the vinyl acetate (VAc) content. Due to its outdoor stability, the photodegradation of EVA and long-term deterioration during its service life have been

Correspondence to: F. Catalina (fcatalina@ictp.csic.es).
Contract grant sponsor: MICINN; contract grant number: MAT2009-09671.
Contract grant sponsor: UAM-CAM; contract grant number: CCG10-UAM/AMB-5411.

studied for others applications[2] such us, cell encapsulant[3,4] and toy industry[5] but also in blends with PVC[6] and PE,[7] in EVA composites with inorganic fillers such us clay,[8] carbon black[9] and carbon nanotubes.[10] Recently, a detailed study of the VAc content effect on UV-ageing was published[11] using EVA containing 14% and 18% of VAc.

In the EVA agricultural application,[1] the opaque effect to infrared radiation (thermicity) is increased. Acetate functionalities have absorption bands in the IR region between 7-14 microns of wavelength and the EVA copolymers with high contents of VAc can be considered thermal- or heat- insulators (according to the UNE-EN regulation 13206). The presence of acetoxy groups in the ethylene prevents adjacent PE chains packing into a crystal lattice; therefore EVA with a Vac content higher than 30% w/w is sensibly amorphous. The less crystalline character of the EVA copolymers improves visible light transmission, reduces turbidness and improves mechanical properties such us impact and tear. Due to these advantages, for some years now, EVA copolymers have shifted polyethylene in agricultural film applications. EVA copolymers with a randomly content of VAc lower than 18% are used as monolayer films since higher contents increase polarity to allow adhesion of powder to the film surface diminishing the necessary transparency for plant growth.

In this paper, we have studied the photodegradation of an EVA copolymer with a content of 9% in vinyl acetate, due to the interest of this grade in agricultural mulching film. Also we have evaluated the effect of calcium and iron stearates as additives on the degradation process. The degradation of these materials has been compared with earlier results obtained with polyethylene[12] using these pro-oxidant additives. Attenuated total reflectance-Fourier Transform Infrared spectroscopy (ATR-FTIR), differential scanning calorimetry (DSC), gel permeation chromatography (GPC), and thermogravimetric analysis (TGA) were used to evaluate the degree of photodegradation of the materials and the effect of the stearates as pro-oxidants.

Chemiluminescence (CL) has been used to study oxidation of the EVA films, due to its offered advantages with respect to many conventional techniques.[13] Chemiluminescence from polymers is due to the recombination of secondary alkyl peroxy radicals, which promotes ketone products to its lowest triplet state and the radiative deactivation gives the light emission in the visible region.[14] The chemiluminescence emission can be related to the hydroperoxide (POOH) content, since generation of peroxy radicals depends on the peroxide concentration formed during processing or in-service life of the material under ambient conditions.[15] Hence, the activity of calcium and iron stearates has been also evaluated by chemiluminescence measurements of EVA-films at different ageing times, and the results were confirmed by analysis of the molecular weight changes and carbonyl index measurements.

After photodegradation, mulching film fragments are difficult of collect from the soil since erosion by wind and rain contribute to complete the breakdown of the embrittled film into friable powder. The objective of total disappearance of the films fragments from the agricultural fields would imply polyethylene biodegradation, known as "oxo-biodegradation". This mechanism of environmental biodegradation is to promote, first, abiotic (photo or thermo) oxidation, and second, microbial biodegradation. Most of the studies on the biodegradability of polyethylene containing pro-oxidants have been carried out on complex solid media such as soil and compost, but only recent research[16–18] supports the idea that such materials are biodegradable.

Following the objective of evaluation of an oxo-biodegradation mechanism, a bacterial biodegradation study (second step) was carried out on the previously (first step) photodegraded EVA films. Biodegradation tests on discoid fragments of EVA films were performed in silica at 45°C with controlled inocula of the bacteria isolated in a previous work[18] from mulching films exposed in a agricultural field, mixture of *Bacillus cereus, Bacillus megaterium, Bacillus subtilis* (MIX). In parallel experiments biodegradation was also studied using *Brevibacillus borstelensis* as reference strain. Together with a characterization study of the biodegraded samples, two different techniques were used to evaluate biodegradation of EVA films, measurement of the carbon dioxide production or mineralization (process where an organic substance is converted to an inorganic product) by indirect impedance and chemiluminescence emission of biodegraded film samples. Both techniques[19,20] were previously employed and proved their suitability to study polymer biodegradation. With this study, the presence of a polar monomer, vinyl acetate, in the polyethylene chain has been evaluated in terms of photodegradation and biodegradation.

EXPERIMENTAL

Materials and polymer characterization

Films of 25 microns of thickness prepared by blow moulding extrusion from a commercial grade (PA-530 from Repsol) ethylene-vinyl acetate copolymer (EVA) of 9% of vinyl acetate content (VAc) and EVA films with iron and calcium stearates (EVA-Fe, EVA-Ca) as pro-oxidant additives (at 0.2% w/w) were prepared by Repsol.

Molecular weight was measured by *Gel Permeation Chromatography* (GPC) on a Polymer Laboratories PL-

GPC 220 apparatus with a differential refractive index detector. The mobile phase was 1,2,4-trichlorobenzene to which 2,6-di-tert-butyl-4-methyl phenol (BHT) antioxidant (0.015%) was added. The analytical flow rate was 1 mL/min and the temperature was 160°C. The values obtained were referenced to a universal curve with the following viscosimetric parameters $K = 3.95 \times 10^{-4}$ and $\alpha = 0.726$ (polyethylene).

FTIR spectra were obtained using a PERKIN ELMER BX-FTIR spectrometer coupled with an Attenuated Total Reflectance (ATR) accessory, MIRacle^{TM}ATR from PIKE Technologies and interferograms were obtained from 32 scans at a 4 cm^{-1} resolution from 400 to 4000 cm^{-1}. Before the actual analysis, background spectra were obtained without samples in the chamber. EVA degradation was determined by using the standard Carbonyl Index method[21] (CI), as the ratio of the optical density of the ketone carbonyl absorption band at 1715 cm^{-1}, and the optical density of the in-plane deformation rocking absorption band of methylene at 2850 cm^{-1} taken as internal thickness band ($CI = A_{1715}/A_{2850}$). Also, CIs referred to other specific bands were calculated such as, ester carbonyl stretching vibration at 1735 cm^{-1} (A_{1735}/A_{2850}), asymmetric and symmetric stretching vibrations (C—O—C) at 1238 and 1175 cm^{-1} respectively (A_{1238}/A_{2850} and A_{1175}/A_{2850}) or lactone carbonyl band at 1780 cm^{-1} (A_{1780}/A_{2850}).

Differential scanning calorimetry (DSC) was performed on a METTLER DSC823 instrument over the temperature range 30°C to 180°C. The measurements were made at a heating rate of 10°C/min in an inert atmosphere of nitrogen and the instrument was calibrated with an indium standard ($T_m = 429$ K, $H_m = 25.75$ J/g). To erase the thermal history of the material, first a heating ramp rate at 10°C/min was used, followed by a cooling ramp and a consecutive heating ramp of 10°C/min each. The melting peak (T_m) and the melting enthalpy (ΔH_m) were obtained, and percentages of crystallinity ($\%X_c$) were determined using the reference of 293 J/g for crystalline polyethylene.[22] For the Oxidation Induction Time (OIT), a standard method (ASTM 3895-80 and ISO 11357) was used to determine the thermal stability of the initial EVA films prepared in this work. The measurement was made with DSC in the isothermal mode at a constant temperature of 200 °C. The sample was maintained under nitrogen (40 mL/min) until the test temperature was attained, and then a flux of oxygen (40 mL/min) was supplied. The latter was taken as time zero. The OIT value is the time needed to reach the onset of oxidation, detected as the start of an exotherm, and can be correlated with the stability of the material.

Thermogravimetric analysis

The TGA experiments have been carried out in a TGA Q-500 (Perkin-Elmer). The heating rate for the dynamic conditions was 10°C/min, and the nitrogen flow was maintained constant at 60 mL/min.

Identification of the degradation products extracted from EVA was undertaken by Gas chromatography mass spectrometry (GC-MS) with a Agilent Technologies 6890 N chromatograph coupled to a *5973 inert* mass spectrometer using helium as the carrier gas, and equipped with an *HP-5MS* capillary column. The oven temperature was programmed from 80 to 250°C (5°C/min), and maintained for 30 min. After that, samples were injected at 250°C. The degradation products were identified by comparing their mass spectrum with the one from the NST database and checked by comparison of the retention times with that of naphthalene as reference sample. For that purpose, the extraction of degradation products from EVA samples was performed using 5 mg of sample, cut into small pieces, mixed with 10 mL chloroform in a 20 mL glass vial and ultrasonicated in a Branson 2210 apparatus for 2 h in a hot water bath held at 60°C. The extract obtained was concentrated by total evaporation of solvent at room temperature. Afterwards, 2 mL of chloroform and 20 µl of stock chloroform-solution of naphthalene (1 g/L) as internal standard were added. The extract was filtered through a 0.2 mm filter prior to analysis[5] by GC-MS.

Chemiluminescence

Chemiluminescence emission of film samples were obtained as described earlier[23] and using a CL400 ChemiLUME apparatus developed by Atlas Electric Devices Co. Samples for chemiluminescence measurements were prepared by cutting circular specimens of 12 mm in diameter from the polymer films; hence the emission area was maintained constant in all the experiments. The film samples were held in aluminum dishes and two different types of tests were performed: A) Isothermal: samples of material are preheated up to the test temperature (170°C) under nitrogen or oxygen, and the temperature of the test maintained constant. B) Dynamic: material samples are heated up with pre-test ramp (2°C/min.) under constant flow of nitrogen (50 mL/min.). Chemiluminescence signal from film samples were collected in a water-cooled photon counting photomultiplier, which was previously calibrated using a radioactive standard provided by Atlas. The data collected were processed using the specific software supplied with the instrument.

Ageing

The accelerated photodegradation of the films was carried out during 432 h (18 days) in a ATLAS/SUNTEST XLS provided with a 2500W Xenon lamp and a solar filter (borosilicate). Incident energy was

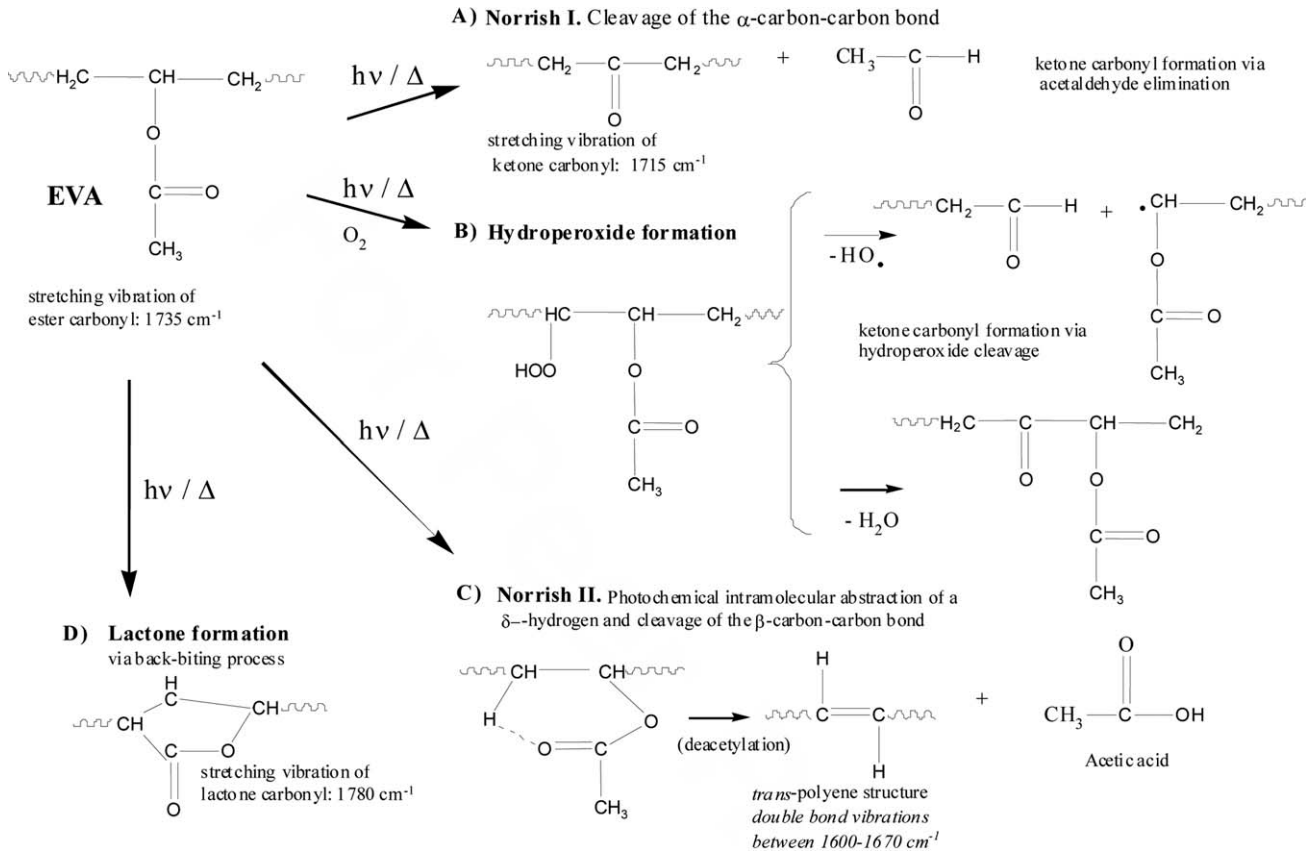

Scheme 1 Degradation mechanisms of ethylene-vinyl acetate copolymers.

fixed at 550 W/m^2 in the interval 300-800 nm using a XenoCal® WB 300-800 irradiance sensor. Temperature was maintained constant at 45°C during the testing program set. Exposed samples were mounted on metallic plates (1 × 4 cm) and were periodically taken out and characterized.

Bioassay procedure and indirect impedance technique

Aerobic biodegradation of polyethylene film samples by bacteria were conducted at 30 and 45°C in bioreactors of 7 mL of capacity, filled with 1 g of sterile silica and 1.5 mL of bacteria suspension in Minimal Growth Medium (MGM) of 2.5 × 10^7 cells/mL of concentration, prepared as detailed before.[24] The composition of MGM used in this work contained: $NH_4H_2PO_4$ 8 g, K_2HPO_4 2 g, $MgSO_4 \cdot 7H_2O$ 0.5 g, $NaSO_4$ 0.5 g, $ZnCl_2 \cdot 2H_2O$ 8 mg, $MnSO_4 \cdot 7H_2O$ 8 mg, $FeSO_4 \cdot 7H_2O$ 10 mg, $CaCl_2$ 0.05 g, distilled water 1000 mL. In this way, a suspension of each bacterium was prepared and in the case of the mixture of *Bacillus*, MIX, equal parts of each suspension were mixed. After that, 10 discs of film samples of 4 mm of diameter (5 mg) were added to the medium. These containers were introduced in disposable cylindrical cells of 20 mL charged with 1.5 mL of 2 g/L KOH aqueous solution and provided by four stainless steel electrodes to measure impedance on a Bac-Trac 4300 (SY-LAB Geräte GmbH, Neupurkerdorf, Austria). The experimental device and procedure were described before.[19] The device monitors the relative change in the initial impedance value of KOH solution which is converted in concentration of carbon dioxide by a calibration curve of impedance variation versus concentration of CO_2. The percentage of biodegradation of the sample can be calculated taking in account the theoretical amount of carbon dioxide ($[CO_2]_{Theor.}$) of the sample, % biodeterioration = $[CO_2]_t \cdot 100/[CO_2]_{Theor.}$

RESULTS AND DISCUSSION

Evaluation of photodegradation of EVA films by ATR-FTIR and chemiluminescence

The infrared spectra of EVA-films show notable changes of characteristic bands corresponding to functional groups which appear with irradiation time. In Scheme 1, the different reactions that take place in the mechanism of EVA-photodegradation are compiled.[11,25]

EVA mulching films prepared in this work were characterized by ATR-FTIR and the relative change in functional groups after 432 h of irradiation are

TABLE I
Carbonyl Index Values of Different Characteristics Bands of EVA (9% of VAc) Containing Ca and Fe Stearates, Initial and After 432 h of Irradiation Time

Film sample	A_{1735}/A_{2850}	A_{1715}/A_{2850}	A_{1238}/A_{2850}	A_{1175}/A_{2850}	A_{1780}/A_{2850}
EVA	0.30	0.03	0.35	0.03	0.01
EVA Photodeg.	0.28	0.10	0.33	0.08	0.02
EVA-Ca	0.53	0.06	0.61	0.06	0.01
EVA-Ca Photodeg.	0.44	0.28	0.53	0.14	0.07
EVA-Fe	0.53	0.07	0.60	0.06	0.01
EVA-Fe Photodeg.	0.44	0.25	0.46	0.17	0.04

reported in Table I. The Carbonyl Index (CI) evolution with photodegradation confirmed the growth of two characteristics absorptions, shoulder at 1715 cm^{-1} and broadband at 1175 cm^{-1}, assigned to ketone carbonyl structure. Ketone groups are formed from vinyl acetate moieties by Norrish I and hydroperoxide cleavage reactions as shown in Scheme 1, A and B respectively. At the same time, a decrease of the ester CI was observed after photodegradation on the ester (acetate) absorption band at 1735 cm^{-1} and the vibration at 1238 cm^{-1} assigned to the asymmetric stretching frequency ν_{as}(C—O—C) of the acetate.[26,27] With the photodegradation of the EVA film a new carbonyl vibration was observed at 1780 cm^{-1} that was assigned[27] to the lactone formation via back-biting process, Scheme 1 reaction D. The presence of Ca and Fe stearates increases the differences of CI after photodegradation.

The evolution of the CI of the 1715 cm^{-1} ketone band with irradiation time is shown in Figure 1. Calcium and iron stearates increased notably the ketone formation via acetaldehyde elimination (Scheme 1A) respect to the pure EVA. This behavior confirms the efficient pro-oxidant effect of the stearates as it was earlier observed in polyethylene.[12]

The analysis of non-isothermal chemiluminescence runs under nitrogen atmosphere for initial and photodegraded samples provides a useful tool to evaluate the activity of stearates as pro-oxidants, both during processing and photoageing of the films, Figure 2.

The CL-temperature curves for pure EVA showed the increase of intensity when the molten state region of the film (above 105°C) is reached. In the melt, the mobility of the peroxy radicals and their bimolecular termination reaction, responsible for the chemiluminescence emission in the polymers, is favoured. In the initial films the presence of pro-oxidants decreased slightly the onset temperature of the CL-emission (EVA-Ca, $T_{CLonset}$ = 160°C; EVA-Fe, $T_{CLonset}$ = 175°C) respect to the pure EVA ($T_{CLonset}$ = 190°C) indicating a higher hydroperoxide formation and slight trend towards oxidation during film processing. The photodegradation of the EVA films after 432 h of irradiation time produced drastic changes on the CL-Intensity profiles and CL emission shifted towards lower temperatures under the EVA melt temperature. The effect of pro-oxidants was evidently significant, and in presence of calcium and iron stearates, the formation of peroxide peaks was observed at lower temperatures, Figure 2. These intense emissions would indicate that higher amounts of hydroperoxides were induced by the

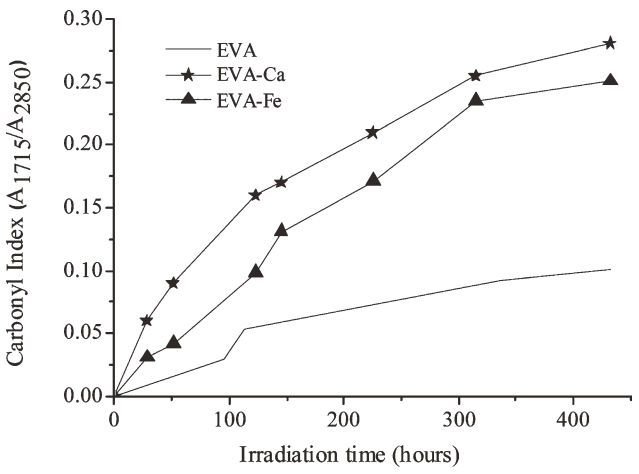

Figure 1 Carbonyl Index profile of ketone carbonyl band of EVA films at different irradiation times.

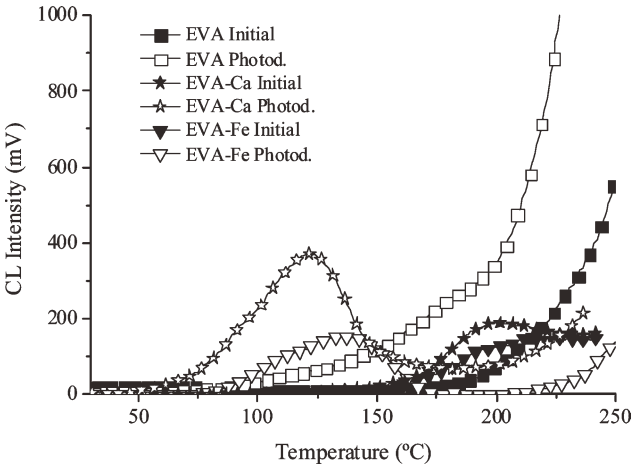

Figure 2 Chemiluminescence temperature-ramping curves obtained for initial and photodegraded (432 h) EVA films under nitrogen.

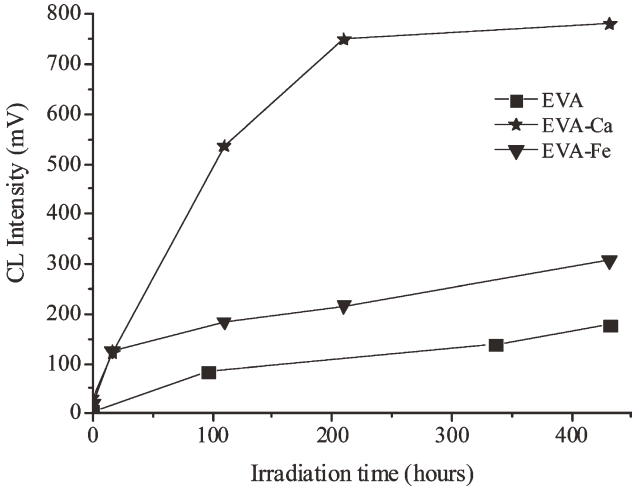

Figure 3 Chemiluminescence intensity determined at 170°C under nitrogen versus photoageing time of EVA films.

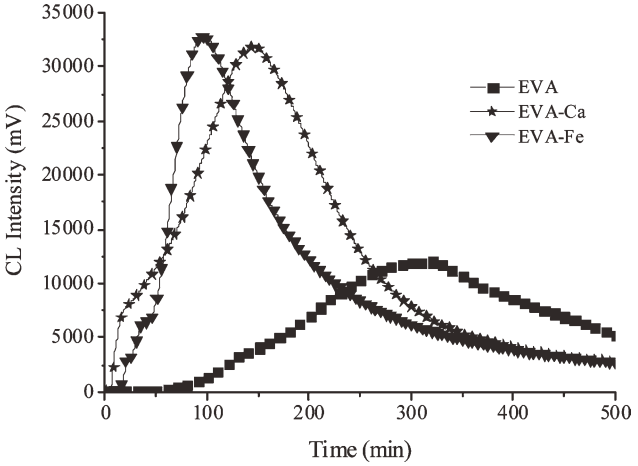

Figure 4 Chemiluminescence curves for initial EVA films obtained at 170°C under oxygen.

action of pro-oxidants during photoageing of the EVA films.

The evolution of CL-Intensity profiles with irradiation time is represented in Figure 3, for the EVA films. The results confirm a higher degree of degradation of samples containing Ca and Fe stearates respect to pure EVA. This higher hydroperoxide formation in the films containing pro-oxidants would be on agreement with the higher content of carbonyl species analyzed by ATR-FTIR, Figure 1.

Also, the activity of pro-oxidants on thermal oxidation of EVA was studied on CL intensity-time runs under oxygen, Figure 4.

The chemiluminescence emission was enhanced with respect to that obtained under nitrogen, since under oxygen the samples were oxidized in a diffusion-controlled reaction simultaneously to the emission. The isothermal CL curves of EVA films exhibited double stage of oxidation, oxygen independent and oxygen diffusion-controlled reactions, with different oxidation rate during the processes, typical of polyethylenes.[28,29] The first maxima appeared as shoulder of the curve as found earlier[12] for polyethylene.[30] The chemiluminescence intensity of second maxima was seen to be highly affected with incorporation of stearates and CL was enhanced and shifted to lower oxidation time respect to pure EVA. This fact can be associated to the decomposition of hydroperoxides catalyzed by the presence of metal ion complexes, leading to the generation of free radicals, which initiate the oxidation[31] of the polyethylene sequences of EVA.

Evaluation of photodegradation of EVA films by thermal analysis

EVA films before and photodegraded, pure and with pro-oxidants, were studied by thermal analysis. EVA films exhibited a single broad endothermic peak profile on DSC before and after 432 h of irradiation. The endotherms started at a low temperature of 60°C, involving no well defined secondary crystallizations and showed a single major melting peak due to the primary crystallization,[32] the data are compiled in Table II. The melting peak temperatures

TABLE II
DSC, TGA, and DTGA Results of EVA Films Initial and After 432 h of Irradiation Time

Film sample	DSC			TGA				DTGA	
	T_m (°C)	χ_c (%)	OIT (s)	T_{onset} (°C)	T_{10} (°C)	T_{50} (°C)	ΔW_1 (%)	T_{st1} (°C)	T_{st2} (°C)
EVA	105	24	170	349	415	460	8.4	359	469
EVA Photodeg.	105	25	–	293	362	450	16.1	358	460
EVA-Ca	103	23	116	349	420	473	9.2	371	479
EVA-Ca Photodeg.	103	28	–	276	356	466	19.7	372	480
EVA-Fe	103	23	117	357	395	478	8.6	371	484
EVA-Fe Photodeg.	103	27.9	–	285	368	472	18.2	369	482

T_m, melting peak of primary crystallization; X_c, percentage of crystallinity; OIT, oxidation induction time; T_{onset}, onset temperature of weight loss (weight loss at 3%); T_{10} and T_{50}, temperatures corresponding to 10 and 50% weight loss respectively; ΔW_1, weight loss in the first stage corresponding to deacetylation; T_{st1} and T_{st2}, temperatures of the maximal degradation rates of stages 1 and 2 respectively; –, not determined.

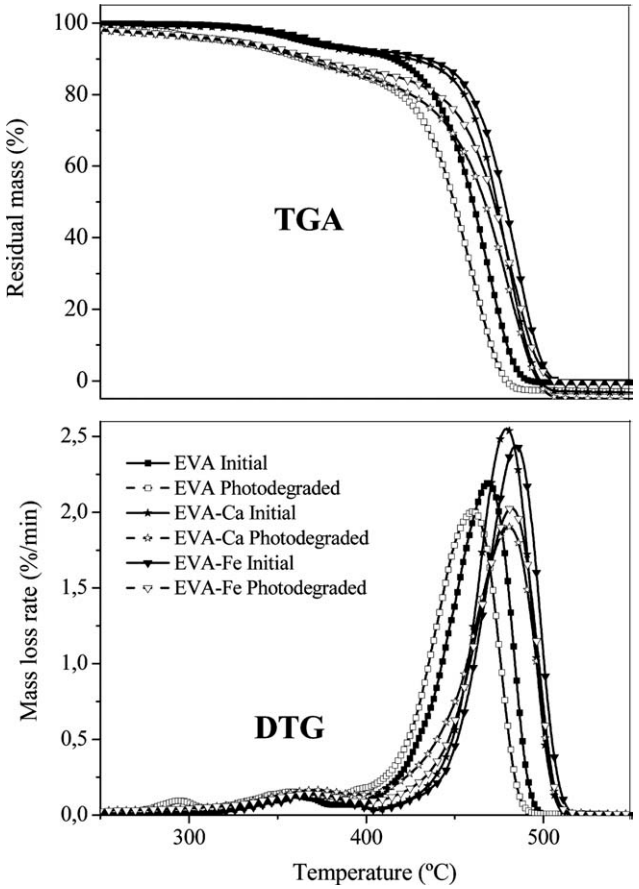

Figure 5 TGA and DTGA thermostability profiles of EVA (9% of VAc) films containing Ca and Fe, initial and photodegraded after 432 h of irradiation time.

remained constant after ageing confirming that the primary crystalline regions of the EVA films are stable and the photodegradation process takes place in the amorphous phase of the material. Photodegradation of EVA samples induced a slight growth in the overall crystallinity (% χ_c), this effect has been reported in EVA by other authors.[11] During ageing, high temperature environment allowed physical annealing of EVA-material[33] and ethylene chain segments of the EVA in the secondary crystallization region are able to re-arrange. The amorphous phase degradation produces less intra/inter-molecular entanglement in macromolecules and also facilitates their re-arrangement or recrystallization during ageing.[34] The lower stability of the films containing pro-oxidants is evidenced by the values of the Oxidation Induction Times (OIT) determined by DSC, Table II.

The thermal stabilities of photodegraded EVAs under nitrogen are shown in Figure 5, where both thermogravimetric (TGA) and derivative thermogravimetric (DTGA) are plotted versus temperature in the Interval 100-550°C.

Two weight loss steps are observed like in poly(-vinyl acetate), the first one under 400°C due to the autocatalytic deacetylation in the acetate fraction of EVA (Norrish II reaction, Scheme 1C) and, the second one, in the interval 400–520°C where the complete chain scission of the residual material takes place. In Table II, all the characteristic parameters of the EVA thermostabilities are compiled. In the initial films, the first weight loss (ΔW_1) of the initial films is close to the 9% of acetate content present in the EVA indicating an efficient deacetylation in the first thermal decomposition stage. After 432 h of irradiation the weight loss in the first stage increases and, in particular, in the materials containing pro-oxidants the values shift from 9.2 to 19.7% on EVA-Ca and from 8.6 to 18.2% on EVA-Fe. In the photodegraded EVA films, deacetylation is accompanied by the elimination of terminal active units on the degraded shorter main-chains of EVA. Jin et al.[11] obtained similar results, in the photodegradation of EVA's of 14 and 18%.

TGA characteristics temperatures in the Onset, 10% and 50% of weight loss decrease in the photodegraded EVAs respect to the initial films confirming that chain scission is the responsible of diminution in thermal stability. The peak position of stage 1 and 2, analyzed by DTGA (T_{st1} and T_{st2}) do not change with photodegradation for each EVA film, indicating that the decrease in molecular weight do not affect the maximum decomposition rate.[11,35]

The photodegradation of the EVA films during 432 h of irradiation decreases the molecular weight as it is evidenced by the GPC data compiled in Table IV. The effect of Ca and Iron stearates produced a drastic reduction of molecular weight of the EVA films.

The increased pro-oxidative ability of iron stearate respect to calcium stearate may be related to the fact that pro-oxidants based on metal combinations capable of yielding two metal ions of similar stability and with oxidation number differing by one unit only exhibited stronger catalytic effect.[36]

In all the solutions prepared with photodegraded materials for GPC analysis, gel formation was detected and the crosslinking level of samples was lower than 5% in agreement with other authors.[4,11,37] Molecular weight measured by GPC refers to non-crosslinked fractions and a decrease in the polydispersity value was observed by GPC (Table IV) in Ca and Fe photodegraded samples, in agreement with similar results published by other authors.[11]

Evaluation of biodegradation by ATR-FTIR, chemiluminescence, and GC-MS product analysis

In previous works of polyethylene biodegradation in the presence of pro-oxidants,[18,38] a drastic effect of temperature was observed in the biodegradation assays. The mineralization of photodegraded

TABLE III
Carbonyl Index Values of Characteristics Bands of EVA-9% of VAc Containing Ca and Fe Stearates, After 432 h of Irradiation and After 90 Days of Bioassay Using a Mixture of *Bacillus* (MIX) and the Bacterium *Brevibacillus borstelensis*

	A_{1735}/A_{2850}			A_{1715}/A_{2850}			A_{1238}/A_{2850}			A_{1175}/A_{2850}		
Film sample	Phot.	MIX	*B.bors.*	Phot.	MIX	*B.bors.*	Phot.	MIX	*B.bors.*	Phot.	MIX	*B.bors.*
EVA	0.28	0.11	0.07	0.10	0.04	0.02	0.33	0.16	0.10	0.08	0.06	0.05
EVA-Ca	0.44	0.08	0.08	0.28	0.06	0.05	0.53	0.11	0.09	0.14	0.08	0.04
EVA-Fe	0.44	0.16	0.10	0.25	0.16	0.03	0.46	0.21	0.14	0.17	0.11	0.08

polyethylenes increased substantially at 45°C being extremely slow at 30°C. For this reason, biodegradation of EVA was only performed at 45°C.

The carbonyl index (CI) values measured by ATR-FTIR for the photodegraded EVA films after 90 days of bacterial biodegradation are summarized in Table III.

Incubation of the photo-oxidized EVA-films with *B. borstelensis* and MIX at 45°C for 90 days showed a marked reduction in the amount of carbonyl groups

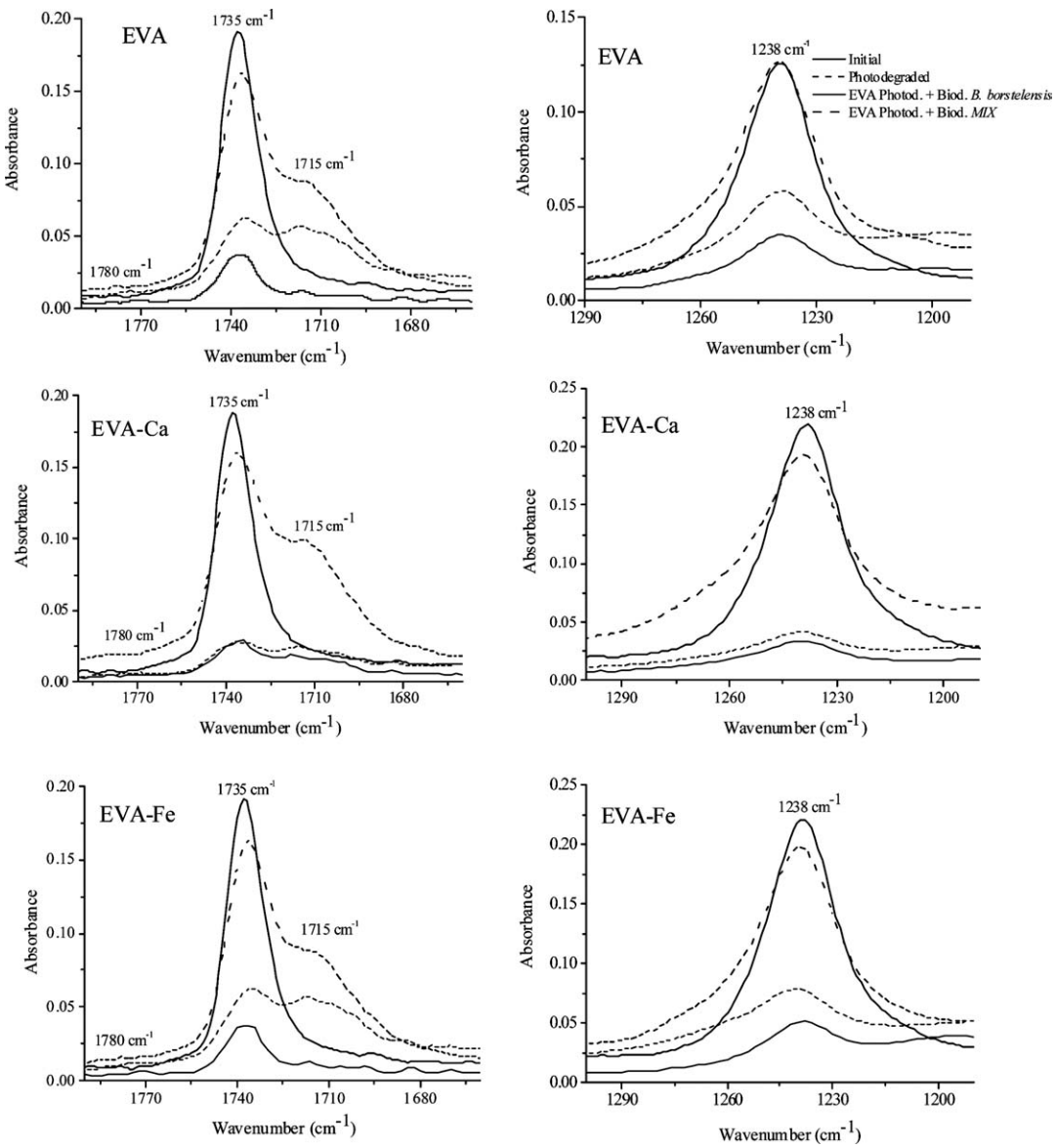

Figure 6 FTIR spectra of EVA films, initial, photodegraded after 432 h of photoageing and after 90 days of bacterial biodegradation at 45°C.

TABLE IV
GPC Data of Number-Average Molecular Weight (M_n), Weight-Average Molecular Weight (M_w), Peak Top Molecular Weight (M_p), and the Polydispersity of Initial, Photodegraded After 432 h of Irradiation, and After 90 Days of Biodegradation by the Mixture of *Bacillus*, MIX

	Initial				Photodegraded				Phot. + Biod. *MIX*			
Simple	M_n	M_w	M_p	PD	M_n	M_w	M_p	PD	M_n	M_w	M_p	PD
EVA	11,060	87,700	28,300	7.9	3430	29,100	5870	8.5	–	–	–	–
EVA-Ca	8530	33,900	18,822	4.0	2800	6680	3710	2.8	2200	51,270	4050	23.2
EVA-Fe	13,600	119,500	38,900	8.8	2280	14,240	3840	6.2	1380	6700	2650	4.8

–, not determined.

estimated in terms of carbonyl index. The percentages of CI decrease are higher when the biodegradation was carried out on higher photodegraded films containing calcium and iron stearates.

The metabolic action at 45°C of *B. borstelensis* and MIX reduced the carbonyl absorption bands in the ATR-FTIR. In Figure 6, the decrease of the carbonyl absorption bands (at 1735 cm^{-1} and 1238 cm^{-1} of the acetate, 1715 cm^{-1} ketone carbonyl and 1780 cm^{-1} lactone carbonyl) is shown for EVA after 90 days of bacterial bioassay together with the corresponding absorption bands of initial and photodegraded films.

The decrease in carbonyl groups on photo-oxidized EVA can be attributed to the preferential microbial assimilation of ester/carbonyl compounds formed during abiotic oxidation. Oxo-biodegradation of polyolefins, like EVA, involves a first step of oxidation followed by a second step of microbial degradation. In this work the biodegradation of EVA chains starts with the photooxidation during the first abiotic step that induced deacetylation and formed hydroperoxides and carbonyl species (ketones) that decreased the molecular weight by chain scission reactions. In Table IV, the changes in molecular weight with biodegradation are compared together with the corresponding photodegraded EVA materials.

After 90 days of biodegradation by the mixture of *Bacillus* MIX, the distribution determined by GPC analysis shifts, Figure 7, toward the left in the present of pro-oxidants, slightly in the case of EVA-Ca and pronounced in the case of EVA-Fe. The biodegraded EVA film sample was not possible to analyze due to the gel formation and the difficulties to filtrate before GPC injection. The effect of gel formation was also observed in biodegraded materials and, in the case of biodegraded EVA-Ca (Table IV) a small amount of gel that pass through the filter contributes to an enormous M_w value.

The values of polydispersity ratio are lower in the biodegraded EVA-Fe indicating that low molecular weight fragments are consumed faster than the higher oxidized fragments.

As expected, increase biodegradation of EVA was observed, since the more chemically oxidized EVA structures are more susceptible to microbial attack as described in polyethylenes. The decrease in number-average molecular weight (M_n) produced by the mixture of *Bacillus* MIX, after 90 days at 45°C, is in the same range interval (EVA-Ca, 22% and EVA-Fe, 40%) than that observed by other authors,[39] 34% on photodegraded LDPE/pro-oxidant system using *B. borstelensis* (90 days liquid culture at 50°C).

The effect of bacterial biodegradation in molecular weight distributions is enhanced by photodegradation and the catalytic effect of calcium and iron stearates on the abiotic degradation step. To confirm the biodegradation of low-molecular weight products generated in the first abiotic step a quantitative analysis of the degradation products was carried out after solvent extraction by ultrasonication.[40] The

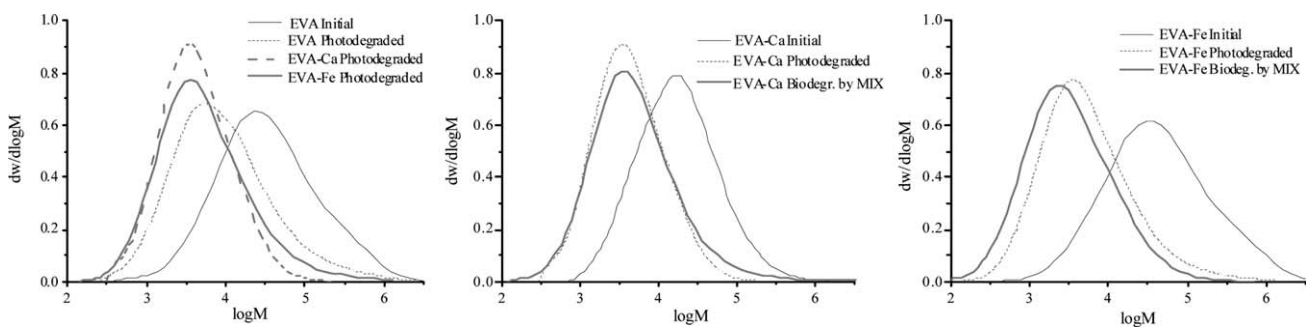

Figure 7 Molecular weight distribution curves determined by GPC of EVA films, initial, photodegraded after 432 h of irradiation and after 90 days of bacterial biodegradation.

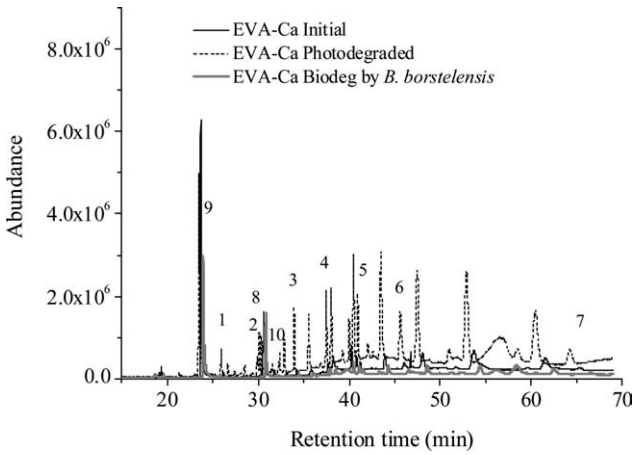

Figure 8 GC-MS chromatogram of the products extracted from initial, photodegraded, and biodegraded EVA films. Different products were identified: (1) Octadecane, (2) Tetracosane, (3) Heptacosane, (4) Eicosane, (5) Octacosane, (6) Nonacosane, (7)Tricontane, (8) Decanol, (9) Tetradecanol, and (10) Octadecanol.

extracted products from EVA film samples, initial, photodegraded (432 h) and after 90 days of biodegradation by bacteria were analyzed by gas chromatography mass spectrometry (GC–MS) for comparison. Similar results were observed using the mixture of *Bacillus* MIX and *B. borstelensis*, the chromatograms obtained using the later bacterium in the biodegradation of EVA-Ca is plotted in Figure 8.

The degradation products extracted and identified from the photodegraded EVA were basically hydrocarbons (saturated and unsaturated) and alcohols of higher molecular weight, as is shown in Figure 8. The hydrocarbons that were present in relatively high concentrations in photodegraded EVA containing pro-oxidants, were found at a significantly lower concentration in EVA without stearates.

After the bacterial treatment at 45°C the low-molecular-weight products were almost absent, at the level present in the initial EVA. This fact is in accordance with the biodegradation mechanism of linear paraffin chains or *n*-alkanes up to tetratetracontane ($C_{44}H_{90}$).[41] Our results confirm that bacteria employed in this work biodegrade extractable low-molecular-weight compounds but also can perturb high-molecular-weight fractions than 5000 Da, which is in agreement with the findings of other authors.[16,18,42,43]

In earlier works, chemiluminescence emissions measured on polymer films were able to quantify the oxidation produced by microorganisms in the structure of gelatin,[20] cellulose triacetate,[44] and photodegraded polyethylene[18] due to their metabolism. The CL emission of EVA-films after 432 h of irradiation and after 90 days of bacterial bioassay was studied by temperature-ramping tests under nitrogen, Figure 9.

The onset of the CL emission shifted toward lower temperatures for the biodegraded samples and in general the intensity of the low-temperature peaks increase. In almost all the biodegraded EVA films containing calcium and iron stearates two peaks emissions were observed (Table II), and their onset temperatures (around 45°C) were significantly lower than that measured for the pure EVA. These results confirm the efficient oxidation activity of the microorganisms at 45°C as observed in polyethylene.[18]

Carbon dioxide production in the biodegradation of EVA films

Biodegradation at 45°C was studied by determining the carbon dioxide produced in the metabolic action of the bacteria, using the indirect impedance technique. The time courses of carbon mineralization at 45°C of the photodegraded EVA films are reported in Figure 10. for the mixture of *Bacillus* (MIX) and *B. borstelensis*.

From the results plotted in Figure 6, biodegradation of photodegraded EVA films started from the beginning of the bioassay and the production of CO_2 was faster when Ca and Fe stearates are present in the formulations. Biodegradation by MIX and *B. borstelensis*

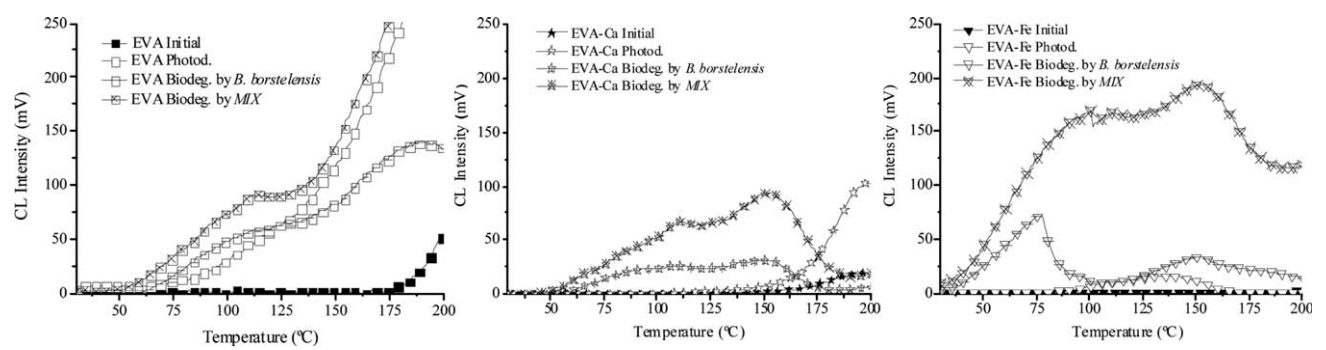

Figure 9 Chemiluminescence temperature-ramping curves obtained from EVA films under nitrogen, initial, photodegraded after 432 h of irradiation and after 90 days of bacterial biodegradation at 45°C.

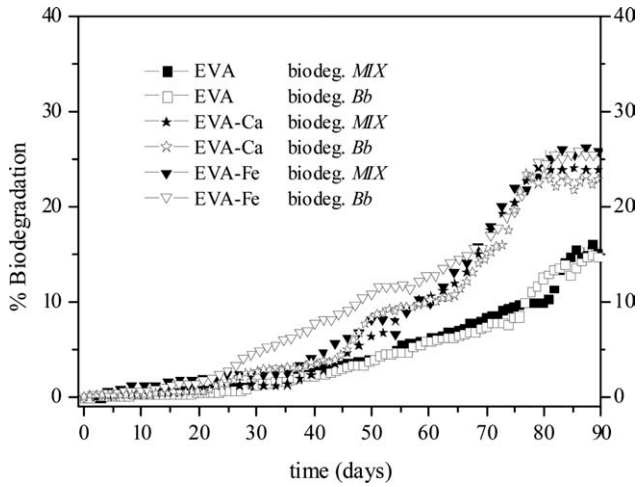

Figure 10 Percentage of carbon mineralization at 45°C, determined from carbon dioxide measurements in the biodegradation of EVA films by the mixture of *Bacillus*, MIX, and *B. borstelensis.*

exhibited a pronounced difference between the pure photodegraded EVA films (around 15% of biodegradation after 90 days) and the corresponding materials containing Ca and Fe pro-oxidants (23–26% of biodegradation after 90 days).

No significant differences were found between both series of bioassays using *B. borstelensis* and the mixture of *Bacillus* MIX on photodegraded EVA films. Only *B. borstelensis* seems to be faster in the mineralization of photodegraded EVA-Fe after the 3 weeks of bioassay but the final percentage of biodegradation was in the same order than that found for the biodegradation of MIX. The percentages of biodegradation reached on photodegraded EVA are higher than the obtained for polyethylene by Hadad et al.[39] and by us[18] using the same bacterial strains, where LDPE mineralization extents reached values of 11.5% with *B. borstelensis* and 7–10% with the mixture of *Bacillus* (MIX).

The percentages of mineralization reported here show that the mixture of *Bacillus* MIX and the bacterium *B. borstelensis* were able to use photodegraded EVA films as the sole carbon source. The nature of EVA in VAc content is important in comparison to polyethylene but the presence of metals and the extent of abiotic degradation of the materials will be crucial to allow a second step in the biodegradation process. We believe that the key factors will be the selection of the microorganisms and the control of the bioassay conditions. It is clear that the presence of random vinyl acetate co-monomer in the polyethylene chain increases the biodegradation extent because of the effectiveness of deacetylation and photo-oxidation processes. The presence of pro-oxidants in the EVA formulations could be an interesting way to prepare more efficient biodegradable materials.

CONCLUSIONS

The photodegradation of EVA films after 432 h of irradiation produced notable changes on the ATR-FTIR spectra. Carbonyl Indexes evolution after irradiation confirmed the growth of ketone carbonyl structures (1715 cm^{-1}) and the appearance of a new band assigned to a lactone generation (1780 cm^{-1}). Simultaneously, a decrease on the ester (acetate) absorption band (1735 cm^{-1}) was observed. The presence of calcium and iron stearates increased the differences of CIs after photodegradation confirming the efficient pro-oxidant effect of these additives.

Photodegradation produced drastic changes on the Chemiluminescence (CL) emission profiles and CL-temperature curves shifted towards lower temperatures and, in particular, when both stearates are present in the EVA-formulations. Under oxygen, isothermal CL-curves of EVA films exhibited double stage of oxidation, typical of polyethylenes.

EVA films were studied by DSC and photodegradation induced a slight growth in the overall crystallinity due to a re-arrangement or recrystallization during ageing. The Oxidation Induction Times determined by DSC confirmed the lower stability of the films containing pro-oxidants.

In the thermograms obtained by TGA, two weight loss steps were observed. The first stage under 400°C, includes deacetylation in the VAc units and, the second one, in the interval 400–520°C is due to decomposition of the material by chain scission. In the photodegraded EVA films deacetylation was accompanied by decomposition of other unstable structures. The molecular weight of the films samples decrease after photodegradation. The presence of Ca and Fe stearates produced a drastic reduction on the M_w of the photodegraded EVA-films.

Biodegradation of photodegraded EVA films were tested at 45°C during 90 days of bacterial treatment with a mixture of *Bacillus* (MIX) and the bacterium *Brevibacillus borstelensis*. The metabolic action of both series of experiments showed a marked reduction in the amount of carbonyl groups estimated in terms of Carbonyl Indexes determined by ATR-FTIR. This bacterial consumption of carbonyl group functionalities on photo-oxidized EVA can be attributed to the preferential microbial assimilation of ester/carbonyl compounds formed during photodegradation. After 90 days of biodegradation by the mixture of *Bacillus* MIX, the molecular weight distribution determined by GPC analysis shift toward low molecular weight, and in particular in the case of EVA-Fe.

The product extracted and identified form EVA films using GC–MS, were present at relatively high

concentrations in photodegraded EVA containing pro-oxidants, but after bacterial treatment, low molecular-weight products were almost absent and at the level of the initial EVA. Bacteria studied in this work employed extractable low-molecular weight compounds as nutrients.

Mineralization of photodegraded EVA-films was studied by determining the carbon dioxide produced in the metabolic action of bacteria, using indirect impedance technique. No significant differences were found between both series of bioassays using *B. borstelensis* and the mixture of *Bacillus* MIX. Biodegradation by these bacteria exhibited a drastic difference between the pure photodegraded EVA film (around 15% of biodegradation after 90 days) and the corresponding materials containing Ca and Fe pro-oxidants (23–26% of biodegradation after 90 days).

The results obtained in this work confirm that the presence of random vinyl acetate co-monomer and the addition of pro-oxidants in the polyethylene chain increase the biodegradation extent because of the effectiveness of deacetylation and photo-oxidation processes.

Also, one of the authors C.A. thanks MICINN for a Ramon y Cajal contract.

References

1. Espí, E.; Fontecha, A.; García-Alonso, Y.; Marín, A.; Salmerón, A. Plasticulture 2004, 123, 72.
2. Gilby, G. W. In Whelan, A.; Lee, K. S., editors. Developments of Rubber Technology-3. London: Applied Science Publishers Ltd.; 1982. p 101, chapter 4.
3. Kojima, T.; Yanagisawa, T. Solar Energy Mater Solar Cells 2004, 81, 119.
4. Ayutthaya, S. I. N.; Wootthikanokkhan, J. J Appl Polym Sci 2008, 107, 3853.
5. Globus, A.; Hornby, G.; Larchev, G.; Hancher, M.; Cannon, H.; Lohn, J. Teleoperated modular robots for lunar operations. Chicago, IL, United states: American Institute of Aeronautics and Astronautics Inc 2004. p. 788–807.
6. Skowronski, T.; Rabek, J. F.; Ranby, B. Polym Eng Sci 1984, 24, 278.
7. Ali, Z. I. J Appl Polym Sci 2007, 104, 2886.
8. Sharif, J.; Dahlan, K. Z. M.; Yunus, W. M. Z. W. Radiat Phys Chem 2007, 76, 1698.
9. Copuroglu, M.; Sen, M. Polym Adv Technol 2005, 16, 61.
10. Morlat-Therias, S.; Fanton, E.; Gardette, J. L.; Peeterbroeck, S.; Alexandre, M.; Dubois, P. Polym Degrad Stab 2007, 92, 1873.
11. Jin, J.; Chen, S.; Zhang, J. Polym Degrad Stab 2010, 95, 25.
12. Pablos, J. L.; Abrusci, C.; Marín, I.; López-Marín, J.; Catalina, F.; Espí, E.; Corrales, T. Polym Degrad Stab 2010, 95, 2057.
13. Peinado, C.; Allen, N. S.; Salvador, E. F.; Corrales, T.; Catalina, F. Polym Degrad Stab 2002, 77, 523.
14. Schard, M. P.; Russel, C. A. J Appl Polym Sci 1964, 8, 985.
15. Kron, A.; Stenberg, B.; Reitberg, T.; Billingham, N. C. Polym Degrad Stab 1996, 53, 119.
16. Chiellini, E.; Corti, A.; Swift, G. Polym Degrad Stab 2003, 81, 341.
17. Jakubowicz, I. Polym Degrad Stab 2003, 80, 39.
18. Abrusci, C.; Pablos, J. L.; Corrales, T.; López-Marín, J.; Marín, I.; Catalina, F. Int Biodet Biodeg 2011, 65, 451.
19. Abrusci, C.; Marquina, D.; Del Amo, A.; Catalina, F. Int Biodet Biodeg 2007, 60, 137.
20. Abrusci, C.; Marquina, D.; Santos, A.; Del Amo, A.; Corrales, T.; Catalina, F. J Photochem Photobiol A: Chem 2007, 185, 188.
21. Rodriguez-Vazquez, M.; Liauw, C. M.; Allen, N. S.; Edge, M.; Fontan, E. Polym Degrad Stab 2006, 91, 154.
22. Flory, P. J.; Vrij, A. J Am Chem Soc 1963, 85, 3548.
23. Catalina, F.; Peinado, C.; Allen, N. S.; Corrales, T. J Polym Sci Part A: Polym Chem 2002, 40, 3312.
24. Abrusci, C.; Martín-González, A.; Del Amo, A.; Corrales, T.; Catalina, F. Polym Degrad Stab 2004, 86, 283.
25. Allen, N. S.; Edge, M.; Rodriguez, M.; Liauw, C. M.; Fontan, E. Polym Degrad Stab 2000, 68, 363.
26. Haken, J. K.; Werner, R. I. Br Polym J 1971, 3, 157.
27. Haslam, J.; Willis, H. A.; Squirrell, D. C. M. Identification and Analysis of Plastics, 2nd ed.; Butterworth: London, 1972, p. 178
28. Zlatkevich, L. J Polym Sci Part B: Polym Phys 1985, 23, 1691.
29. Broska, R.; Rychly, J. Polym Degrad Stab 2001, 72, 271.
30. Corrales, T.; Escudero, M.; Quijada, R.; Catalina, F.; Abrusci, C. Eur Polym J 2009, 45, 2708.
31. Jirackova-Audouin, L.; Verdu, J. J Polym Sci Part A: Polym Chem 1987, 25, 1205.
32. Brogly, M.; Nardin, M.; Schultz, J. J Appl Polym Sci 1997, 64, 1903.
33. Chen, S. J.; Zhang, J.; Su, J. J Appl Polym Sci 2009, 112, 1166.
34. Liu, M.; Horrocks, A. R.; Hall, M. E. Polym Degrad Stab 1995, 49, 151.
35. Zhao, W.; Zhong, X.; Yu, L.; Zhang, Y.; Sun, J. Polymers 1994, 35, 3348.
36. Jakubowicz, I. Polym Degrad Stab 2003, 80, 39.
37. Yao, D. H.; Qu, B. J.; Wu, Q. H. Polym Eng Sci 2007, 47, 1761.
38. Fontanella, S.; Bonhomme, S.; Koutny, M.; Husarova, L.; Brusson, J. M.; Courdavault, J. P.; Pitteri, S.; Samuel, G.; Pichon, G.; Lemaire, J.; Delort, A. M. Polym Degrad Stab 2010, 95, 1011.
39. Hadad, D.; Geresh, S.; Sivan, A. J Appl Microbiol 2005, 98, 1093.
40. Contat-Rodrigo, L.; Haider, N.; Ribes-Greus, A.; Karlsson, S. J Polym Sci 2001, 79, 1101.
41. Haines, J. R.; Alexander, M. Appl Microbiol 1975, 28, 1084.
42. Roy, P. K.; Titus, S.; Surekha, P.; Tulsi, E.; Deshmukh, C.; Rajagopal, C. Polym Degrad Stab 2008, 93, 1917.
43. Kawai, F.; Watanabe, M.; Shibata, M.; Yokoyama, S.; Sudate, Y.; Hayashi, S. Polym Degrad Stab 2004, 86, 105.
44. Abrusci, C.; Marquina, D.; Santos, A.; Del Amo, A.; Corrales, T.; Catalina, F. Int Biodet Biodeg 2009, 63, 759.